

An SVD-Based Grayscale Image Quality Measure for Local and Global Assessment

Aleksandr Shnayderman, Alexander Gusev, and Ahmet M. Eskicioglu

Abstract—The important criteria used in subjective evaluation of distorted images include the amount of distortion, the type of distortion, and the distribution of error. An ideal image quality measure should, therefore, be able to mimic the human observer. We present a new grayscale image quality measure that can be used as a graphical or a scalar measure to predict the distortion introduced by a wide range of noise sources. Based on singular value decomposition, it reliably measures the distortion not only within a distortion type at different distortion levels, but also across different distortion types. The measure was applied to five test images (airplane, boat, goldhill, Lena, and peppers) using six types of distortion (JPEG, JPEG 2000, Gaussian blur, Gaussian noise, sharpening, and DC-shifting), each with five distortion levels. Its performance is compared with PSNR and two recent measures.

Index Terms—Image quality, local error measurement, objective measures, peak signal-to-noise ratio (PSNR), singular value decomposition (SVD), subjective evaluation.

I. INTRODUCTION

MEASUREMENT of image quality is a challenging problem in many image processing fields from image compression to printing. Over the past 30 years, a vast literature has appeared with many approaches attempting to provide a solution [1]. The image quality measures in the literature can be classified into two groups: subjective and objective [2]. Subjective evaluation is cumbersome as the human observers can be influenced by several critical factors including the environmental conditions, motivation, and mood. The objective measures include bivariate measures such as the mean-squared error (MSE) or L_p -norm [3]–[6], measures mimicking the human visual system (HVS) [4], [7]–[35], and graphical measures [33], [36]–[43]. Furthermore, several papers present comparative evaluations of a number of selected measures for image compression [14], [16], [28], [31], [40], [44], and for noise and blur [13], [45]. The most common objective evaluation tool, the MSE, is very unreliable, resulting in poor correlation with the HVS. In spite of their complicated algorithms, the HVS-based objective measures do not appear to be superior to the simple pixel-based measures like the MSE, peak signal-to-noise ratio (PSNR), or root MSE (RMSE).

Manuscript received October 1, 2003; revised February 21, 2005. This work was supported in part by the Professional Staff Congress (PSC), The City University of New York (CUNY) Research Award 2003-2004. The associate editor coordinating the review of this manuscript and approving it for publication was Dr. Reiner Eschbach.

The authors were with the Department of Computer and Information Science, Brooklyn College, City University of New York, Brooklyn, NY 11210 USA. They are now with the University of North Texas, Denton, TX 76203 USA (e-mail: sanyok01@yahoo.com; eskicioglu@sci.brooklyn.cuny.edu).

Digital Object Identifier 10.1109/TIP.2005.860605

A number of researchers point to the disadvantages of the measures that incorporate an HVS model. Fuhrmann *et al.* [44] discourage the use of metrics based on the spatial frequency properties of the HVS as they require precise knowledge of the viewing conditions. Franti [30] argues that the distortion measure should be independent of the factors such as the compression method used, basic image processing operations, and the viewing distance. According to Wang and Bovik [34], although the viewing conditions play an important role in human perception of image quality, they are not fixed in most cases, and the specific data is generally unavailable to the image analysis system.

An ideal image quality measure should be able to describe 1) the amount of distortion, 2) the type of distortion, and 3) the distribution of error. Such a measure is expected to provide accurate predictions of quality not only at distortion ranges near the visual threshold but also when distortions are significantly above the visual threshold. Undoubtedly, there is a need for an objective measure that provides more information than a single numerical value. Assessment of image quality is an open problem today.

In their 1982 paper [11], Lukas and Budrikis talk about a possible improvement in quality prediction if local rather than global averaging procedures are used. They believe local error measures are particularly pertinent in the case of coding schemes that introduce distortion that is very localized in nature. Westen *et al.* [24] present a perceptual error measure (PEM) based on a multiple channel HVS for use in digital image compression. PEM combines the responses in different frequency bands, orientations and positions. Combination of the responses at each position results in an image with values that represent a local visibility of distortions. In coding applications, the authors believe, such a local measure of image quality is probably more useful than a global one. Eude and Mayache [31] compare four metrics to evaluate the quality of JPEG-compressed images. They conclude by stating that as these metrics do not take into account typical artifacts of other compression methods, a multidimensional measure, with each dimension being related to an artifact, would be an attractive solution.

A recent paper [34] presents a new numerical measure for gray scale images, called the universal image quality index (UQI). The dynamic range of UQI is $[-1,1]$, with the best value achieved when $y_i = x_i$, $i = 1, 2, \dots, n$. As described in the paper, this index models any distortion as a combination of three different factors: loss of correlation, mean distortion, and variance distortion. The index is computed using a sliding window approach with a window size of 8×8 , leading to a quality map of the image. The overall quality index is the

average of all the UQI values in the quality map. The UQI produces unstable results when either of the terms in the denominator is very close to zero. To avoid this problem, the measure has been generalized to the Structural Similarity Index (SSIM) [46]. Q is a special case of SSIM that can be derived by setting C_1 and C_2 to 0. As in the case of UQI, the overall image quality MSSIM is obtained by computing the average of SSIM values over all windows.

Measures that require both the original (reference) image and the distorted image are called “full-reference” methods while those that do not require the original image are called “no-reference” methods. The relevant literature includes several transform-based approaches for developing an image quality measure.

- *Discrete Wavelet Transformation* [33], [47]: A full-reference measure [33] based on integer wavelet transformation presents a graphical representation of image distortion using relative wavelet subband energy. The proposed measure can also be represented as a single numerical value by computing a weighted sum of the subband values. The distortion types for grayscale images are blur, noise, and lossy compression (JPEG, wavelet, and vector quantization). A more recent wavelet-based full-reference distortion measure [47] utilizes linear-phase wavelets (namely, biorthogonal Daubechies 9/7 and cubic spline wavelets). The measure is tested with three types of degradation: Gaussian noise, JPEG compression, and a grid pattern.
- *Fast Fourier Transform* [48]: A no-reference scalar measure that estimates horizontal and vertical blocking artifacts in images. The overall blockiness of the distorted image is given by the arithmetic mean of the two estimates. JPEG compressed grayscale images are used to test the measure. Because of the computational requirements of the FFT, a pixel domain approach was also proposed [49].
- *Discrete Cosine Transform (DCT)*[50]: A no-reference scalar measure that defines a new block across any two adjacent blocks in horizontal and vertical directions. Computations on these overlap blocks result in a map of artifact visibility for the whole image. The set of values in the map can be combined to have a numerical value predicting the overall image quality. The proposed measure is applied to JPEG compressed grayscale images.

In this paper, we explore the feasibility of singular value decomposition (SVD) in developing a new measure that can express the quality of distorted images either graphically [as a two-dimensional (2-D) measure] or numerically (as a scalar measure) both near and above the visual threshold. Our experiments show that the SVD-based measure outperforms PSNR, UQI and MSSIM (two state-of-the-art metrics), consistently measuring the distortion both across different distortion types, and within a given distortion type at different distortion levels.

II. NEW SVD-BASED MEASURE

Every real matrix A can be decomposed into a product of three matrices $A = USV^T$, where U and V are orthogonal ma-

trices, $U^T U = I$, $V^T V = I$, and $S = \text{diag}(s_1, s_2, \dots)$. The diagonal entries of S are called the singular values of A , the columns of U are called the left singular vectors of A , and the columns of V are called the right singular vectors of A . This decomposition is known as the SVD of A [51]. It is one of the most useful tools of linear algebra with several applications to multimedia including image compression [52] and watermarking [53]–[55].

We will restrict our description to gray scale images although generalization to color images is possible. A common approach used for color images is to separate the luminance information (luminance channel Y) from the color information (two chrominance channels U and V), and use the luminance layer only [46].

Every gray scale image can be considered to be a matrix with an integer number corresponding to each pixel. If the SVD is applied to the full images, we obtain a global measure whereas if a smaller block (e.g., 8×8) is used, we compute the local error in that block. An alternative for the global measure is to obtain the local errors in smaller blocks, and average them in a certain way.

A. Graphical Measure

The proposed graphical measure is a bivariate measure that computes the distance between the singular values of the original image block and the singular values of the distorted image block

$$D_i = \text{Sqrt} \left[\sum_{i=1}^n (s_i - \hat{s}_i)^2 \right]$$

where s_i is the singular values of the original block, \hat{s}_i is the singular values of the distorted block, and n is the block size. If the image size is k , we have $(k/n) \times (k/n)$ blocks. The set of distances, when displayed in a graph, represents a “distortion map.” The block size used in our experiments is 8×8 for two reasons: It is a common block size in JPEG compression and other image processing applications, and more importantly, both UQI and MSSIM use a window size of 8×8 .

We applied the measure to five 512×512 grayscale images given in Fig. 1. The distortion types, the distortion levels and the associated parameters are shown in Table I. The JPEG, JPEG 2000, and sharpened images were created using XnView, and the blurred and noisy images were created using Adobe Photoshop. The DC-shifted images were obtained through programming by shifting each pixel by the indicated amount. The parameters in Table I for JPEG and JPEG 2000 are compression ratios whereas the parameters for Gaussian blur, Gaussian noise, and sharpening are obtained from the respective image processing tools (XnView for Windows Version 1.70 and Adobe Photoshop 7.0).

We begin with the observation that an 8-bit black image of size n with pixels values equal to 0 have n singular values that are equal to 0, and a white image of size n with pixels values equal to 255 have one singular value that is equal to $n \times 255$, and $n - 1$ singular values that are equal to 0. We divided the test image Lena into 8×8 blocks, and for each block



Fig. 1. Test images.

TABLE I
DISTORTION TYPES AND LEVELS

| Type \ Level | Level 1 | Level 2 | Level 3 | Level 4 | Level 5 |
|--------------|---------|---------|---------|---------|---------|
| JPEG | 10:1 | 20:1 | 30:1 | 40:1 | 50:1 |
| JPEG2000 | 10:1 | 20:1 | 30:1 | 40:1 | 50:1 |
| G. blur | 1 | 2 | 3 | 4 | 5 |
| G. noise | 3 | 6 | 9 | 12 | 15 |
| Sharpening | 10 | 20 | 30 | 40 | 50 |
| DC-shifting | 4 | 8 | 12 | 16 | 20 |

obtained the ratio between the largest singular value and the second largest singular value. The blocks with the largest and smallest ratios in the whole image are given in Fig. 2. The coordinates of the higher frequency block are (35,16), and the coordinates of the lower frequency block are (45,64). As the range of singular values in a given block depends on the activity level in the block, we propose to use all the singular values in the graphical measure.

In Fig. 3, we present the results for our graphical measure only for Lena. Each distortion map, which provides the amount of distortion, the type of distortion, and the distribution of error, is obtained as a grayscale image by mapping the D_i values to the range [0,255]. Note that the size of a distortion map is 64×64 . We enlarged the maps to make the pixel values more visible; the darker and lighter areas indicate the smaller and larger differences, respectively.

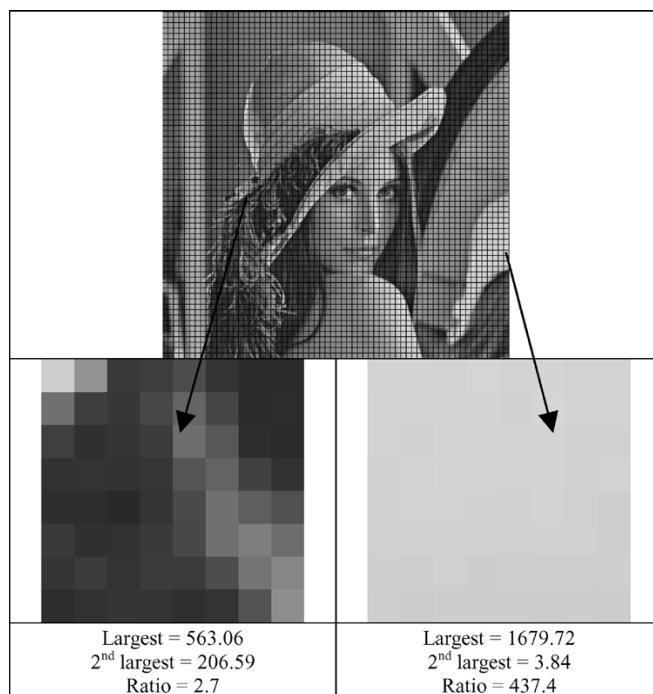


Fig. 2. Lena blocks with the largest and smallest ratios.

We have the following observations based on the distortion maps in Fig. 3.

- JPEG: As the distortion level is increased, the image becomes blocky (which is the major artifact for DCT-based JPEG compression). This artifact becomes visible in the maps starting from compression ratio 30:1, especially on Lena's shoulder and the wall.
- JPEG2000: As this new compression standard is based on the wavelet transform, the images become blurry along the edges, and in high frequency areas. As we increase the compression ratio, the maps display how the image loses its fidelity. When compared with JPEG, this technology is superior especially at higher compression ratios.
- Gaussian blur: This type of distortion substantially affects the edges and high frequency areas, resulting in seriously blurred images. As the radius of blurring is increased, we see high peaks in the maps along the edges, and high frequency areas.
- Gaussian noise: The effect is a uniformly distributed noise across the image which is depicted in the maps as the amount of noise goes up. The noise is visible in high frequency, low frequency, and textured areas.
- Sharpening: This type of filter makes the textured and high frequency areas sharper and crisper. The maps show the distortion in the affected areas. In contrast, sharpening does not introduce noticeable noise in the low frequency areas.
- DC-shifting: If a constant value is added to all the pixel values, the image becomes uniformly lighter, and if a constant value is subtracted from all the pixel values, the image becomes uniformly darker. Because of the range of pixel values of Lena (24–245), we subtracted values that resulted in darker areas along the edges with a sharp

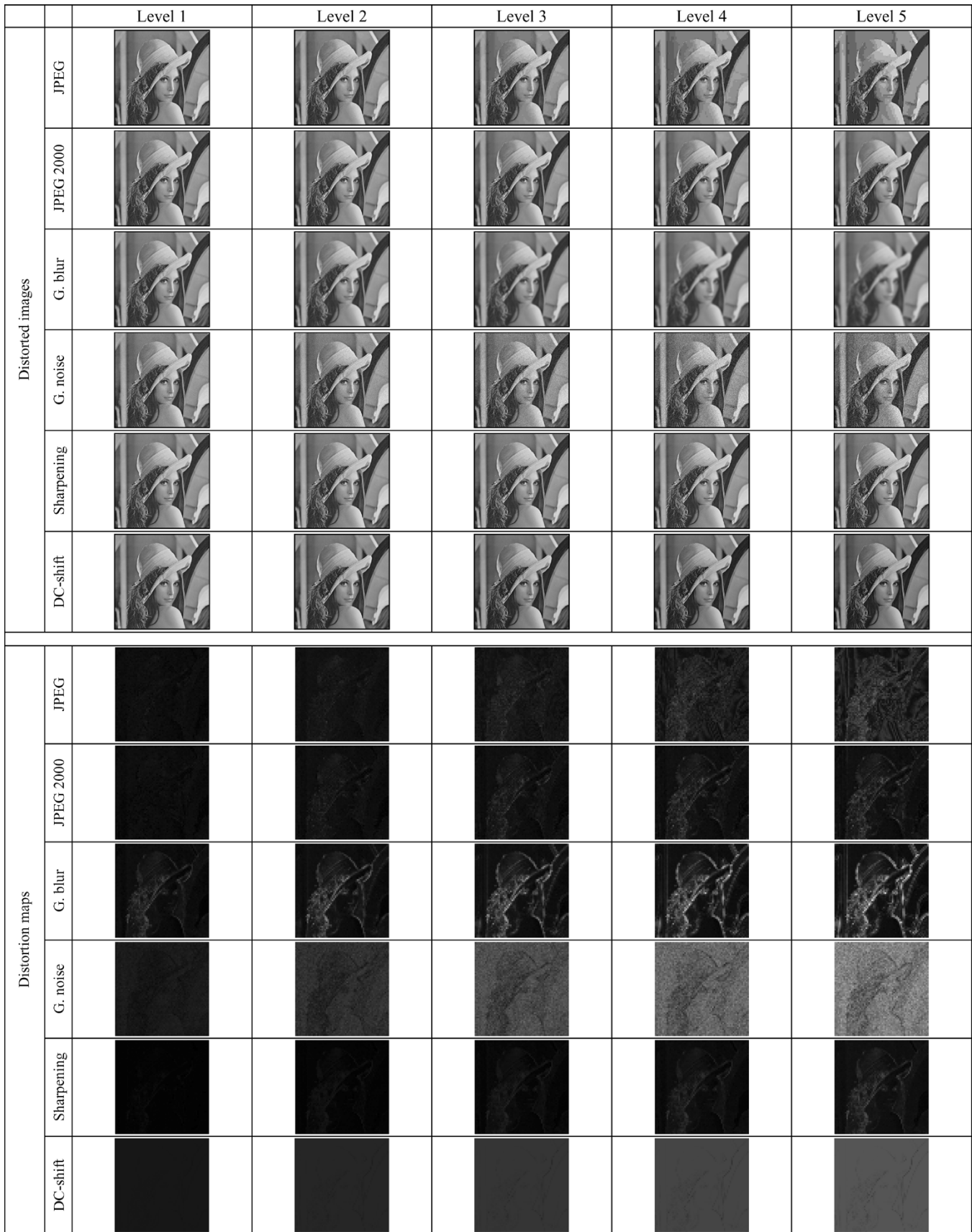


Fig. 3. Distorted images and corresponding distortion maps.

contrast. As smaller pixel values led to smaller singular values, our measure computed smaller differences along

those edges, resulting in “grooves” in the maps. In the other areas, the distribution of distortion is uniform.

B. Numerical Measure

The numerical measure is derived from the graphical measure. It computes the global error expressed as a single numerical value depending on the distortion type

$$\text{M-SVD} = \frac{\sum_{i=1}^{(k/n) \times (k/n)} |D_i - D_{\text{mid}}|}{\left(\frac{k}{n}\right) \times \left(\frac{k}{n}\right)}$$

where D_{mid} represents the mid point of the sorted D_i s, k is the image size, and n is the block size. We will compare its performance with commonly used PSNR, and two state-of-the-art quality metrics, UQI and MSSIM.

Each test image was distorted by six types of noise at five levels, resulting in 30 distorted images. High quality print-outs of each set of distorted images were subjectively evaluated by approximately 15 observers. The printer was a Hewlett-Packard printer with model number "hp color Laserjet 4600dn." The 8-2/16" \times 8-2/16" images were printed on 8.5" \times 11" white paper with basis weight 20 lb and brightness 84. In this experiment, the observers were chosen among the undergraduate/graduate students and professors from the Department of Computer and Information Science at Brooklyn College. About half of the observers were familiar with image processing, and the others only had computer science background. They were asked to rate the images using a 50-point scale in two ways: Within a given distortion type (i.e., rating of the five distorted images), and across six distortion types (i.e., rating of the six distorted images for each distortion level). For each test image, we displayed the 30 distorted images (six distortion types and five distortion levels) with the original image, and asked the observers to rate them. As the proposed measure is not HVS-based, no viewing distance was imposed on the observers in the experiment. Grade 1 was assigned to the best image, and grade 50 was assigned to the worst image.

In the Video Quality Experts Group (VQEG) Phase I testing and validation, a nonlinear mapping between the objective model outputs and subjective quality ratings was used [56]. The performance of the 9 proponent models was evaluated after compensating for the nonlinearity. In this paper, we follow the same procedure by fitting a logistic curve to establish a nonlinear mapping. The logistic function has the form

$$\text{logistic}(\tau, x) = \frac{1}{2} - \frac{1}{1 + \exp(\tau x)}$$

where τ is a constant parameter. Fig. 4 shows the curves fitted for all the four measures compared.

Table II displays the overall performance of the measures using two criteria: Correlation and RMSE between MOS and objective prediction. It can be observed that M-SVD outperforms all three measures. In particular, the correlation is improved by approximately 10%, and the RMSE is reduced by almost 50%, relative to the state-of-the-art metrics UQI and MSSIM.

The real success of objective quality assessment can be determined by predicting the quality not only within a given distortion type but also across different distortion types. So, we also

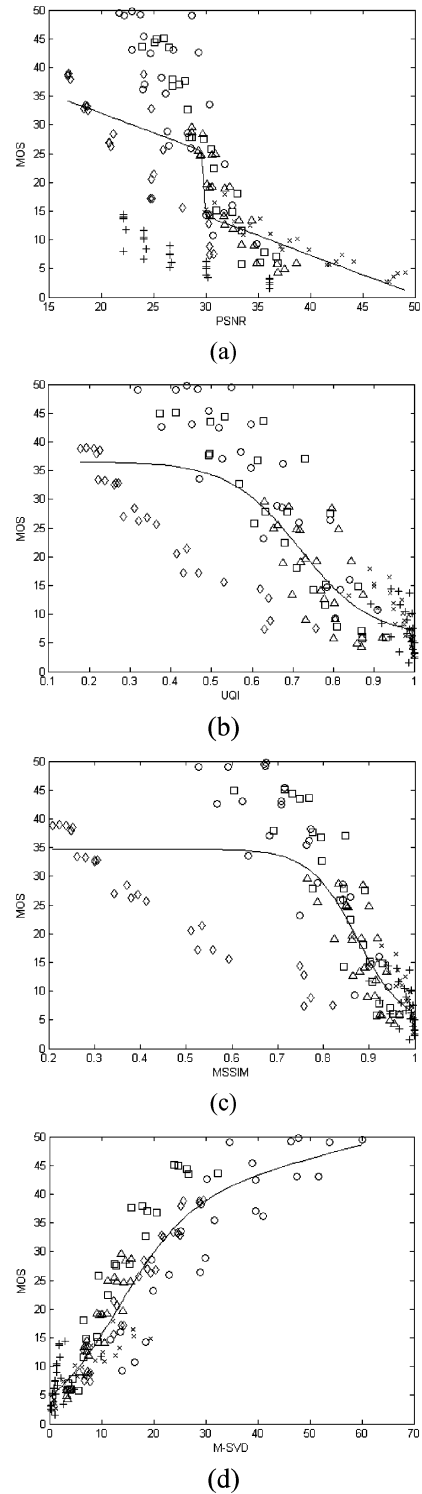


Fig. 4. Comparison of the scatter plots for PSNR, UQI, MSSIM, and M-SVD. MOS is the mean opinion score, and each mark represents one distorted image. The mapping between the distortion types and the marks is as follows: JPEG (\square), JPEG2000 (\triangle), Gaussian blur (\circ), Gaussian noise (\diamond), sharpening (\times), and DC-shifting ($+$).

computed two additional sets of data in comparing the performance of the four measures:

- CC and RMSE within each of the six distortion types;
- CC and RMSE across each of the five distortion levels.

TABLE II
COMPARISON OF FOUR MEASURES

| Criteria\ Measure | PSNR | UQI | MSSIM | M-SVD |
|-------------------|-------|-------|-------|-------|
| CC | 0.697 | 0.839 | 0.833 | 0.928 |
| RMSE | 9.71 | 7.36 | 7.49 | 5.04 |

TABLE III
(A) CC-BASED PERFORMANCE WITHIN EACH DISTORTION TYPE.
(B) RMSE-BASED PERFORMANCE WITHIN EACH DISTORTION TYPE

(a)

| Distortion type\ Measure | PSNR | UQI | MSSIM | M-SVD |
|--------------------------|-------|-------|-------|-------|
| JPEG | 0.974 | 0.904 | 0.928 | 0.977 |
| JPEG2000 | 0.949 | 0.688 | 0.801 | 0.952 |
| Gaussian blur | 0.816 | 0.917 | 0.906 | 0.929 |
| Gaussian noise | 0.901 | 0.984 | 0.987 | 0.975 |
| Sharpening | 0.955 | 0.908 | 0.947 | 0.937 |
| DC-shifting | 0.914 | 0.637 | 0.643 | 0.718 |

(b)

| Distortion type\ Measure | PSNR | UQI | MSSIM | M-SVD |
|--------------------------|------|------|-------|-------|
| JPEG | 3.17 | 5.93 | 5.17 | 2.99 |
| JPEG2000 | 2.56 | 5.91 | 4.88 | 2.49 |
| Gaussian blur | 7.47 | 5.17 | 5.47 | 4.77 |
| Gaussian noise | 4.47 | 1.83 | 1.66 | 2.29 |
| Sharpening | 1.29 | 1.83 | 1.39 | 1.52 |
| DC-shifting | 1.53 | 2.91 | 2.89 | 2.63 |

TABLE IV
(A) CC-BASED PERFORMANCE ACROSS EACH DISTORTION LEVEL.
(B) RMSE-BASED PERFORMANCE ACROSS EACH DISTORTION LEVEL

(a)

| Distortion level\ Measure | PSNR | UQI | MSSIM | M-SVD |
|---------------------------|-------|-------|-------|-------|
| 1 | 0.808 | 0.744 | 0.781 | 0.890 |
| 2 | 0.751 | 0.808 | 0.853 | 0.954 |
| 3 | 0.529 | 0.885 | 0.910 | 0.962 |
| 4 | 0.369 | 0.914 | 0.929 | 0.958 |
| 5 | 0.439 | 0.940 | 0.947 | 0.924 |

(b)

| Distortion level\ Measure | PSNR | UQI | MSSIM | M-SVD |
|---------------------------|-------|------|-------|-------|
| 1 | 2.37 | 2.69 | 2.52 | 1.83 |
| 2 | 5.04 | 4.50 | 3.99 | 2.28 |
| 3 | 8.88 | 4.88 | 4.34 | 2.86 |
| 4 | 11.64 | 5.11 | 4.67 | 3.60 |
| 5 | 12.68 | 4.80 | 4.50 | 5.35 |

The performance results are given in Tables III and IV. We observe that the performance of M-SVD is considerably more consistent across distortion types and across distortion levels. The difference is more pronounced in Table IV which represents an extremely challenging measurement problem. Although PSNR

TABLE V
SENSITIVITY OF M-SVD TO THE BLOCK SIZE

| Criteria \ Block size | 4 | 8 | 16 |
|-----------------------|-------|-------|-------|
| CC | 0.950 | 0.928 | 0.853 |
| RMSE | 2.72 | 5.04 | 7.07 |

outperforms UQI and MSSIM in general with respect to the distortion types, it displays the poorest prediction as the distortion level is raised.

We also analyzed the sensitivity of M-SVD to the block size. Smaller block size results in more detailed distortion maps leading to higher correlation with subjective evaluation. Similarly, larger block size results in coarser distortion maps leading to lower correlation with subjective evaluation. The overall performance of the measure for three block sizes is given in Table V.

III. CONCLUSION

We presented a new image quality measure that can be used graphically as a 2-D tool or numerically as a scalar metric. Our observations regarding the proposed measure are as follows.

- The graphical measure consistently displays the type and amount of distortion as well as the distribution of error in all the images. In the experiments, we used a wide range of distortion types including compression, blur, noise, sharpening and shifting. Some other measures have limited scope as they focus on a particular technology such as image compression [24]–[26], [29]–[31], [44].
- The numerical measure is a derivation from the graphical measure which is expressed as a Minkowski metric $(\sum_k |s_k - \hat{s}_k|^\beta)^{1/\beta}$, where $\beta = 2$, and the image components s_k and \hat{s}_k represent the SVD singular values of the original and distorted images, respectively. It computes a global estimate of the distortion in the image. The subjective evaluation shows that its overall performance is substantially more successful than those of Q and SSIM for six distortion types and five distortion levels.
- Neither the graphical measure nor the numerical measure requires a simplified model of the HVS, necessitating undue computations. Hence, they do not have any assumptions concerning the viewing distance, or the distortion type.
- In some global metrics, the statistics obtained about the impairments in a distorted image are combined in a weighted sum to represent the average error. This weighting is usually problematic as no systematic method is known to determine the weights. Researchers have resorted to simple addition of errors [25], Minkowski metric with different values of β [28], linear combination of distortion factors [22], [29], [30], [33], nonlinear combination of vertical and horizontal features [49], and nonlinear response in different frequency bands, orientations and positions [24]. These efforts may result in different weights for different distortions or image types.

The M-SVD, however, does not require any analysis to compute a weighted sum in predicting the overall error.

- The SVD is of order $O(n^3)$, which makes the computations slower for larger image sizes. If the image is segmented into smaller blocks, and the SVD is applied to each block, the total processing time is much lower. As we use 8×8 blocks, computational requirements are reasonable.
- The smallest parameters in Table I correspond to distortions that are barely visible, and the larger parameters to distortions where the observer preferences start deviating. Hence, the measure is able to reliably predict visual quality not only near the visual threshold but also well above the visual threshold.

To the best of our knowledge, such a generalized objective metric that can be used for local and global measurements does not exist in the current literature. We plan to continue this research by extending the proposed measure to color images, video sequences, and watermarked images.

REFERENCES

- [1] A. M. Eskicioglu, "Quality measurement for monochrome compressed images in the past 25 years," in *Proc. IEEE Int. Conf. Acoustics, Speech, Signal Processing*, vol. 4, Istanbul, Turkey, Jun. 2000, pp. 1907–1910.
- [2] A. M. Eskicioglu and P. S. Fisher, "A survey of image quality measures for gray scale image compression," in *Proc. Space and Earth Science Data Compression Workshop*, Snowbird, UT, Apr. 1993, pp. 49–61.
- [3] W. K. Pratt, *Digital Image Processing*. New York: Wiley, 1978.
- [4] J. O. Limb, "Distortion criteria of the human viewer," *IEEE Trans. Syst., Man, Cybern.*, vol. SMC-9, no. 6, pp. 778–793, Dec. 1979.
- [5] H. L. Snyder, "Image quality: Measures and visual performance," in *Flat-Panel Displays and CRTs*, L. E. Tannas Jr., Ed. New York: Van Nostrand Reinhold, 1985, pp. 70–90.
- [6] A. K. Jain, *Fundamentals of Digital Image Processing*. Englewood Cliffs, NJ: Prentice-Hall, 1989.
- [7] J. L. Mannos and D. J. Sakrison, "The effects of a visual fidelity criterion on the encoding of images," *IEEE Trans. Inf. Theory*, vol. 20, no. 4, pp. 525–536, Jul. 1974.
- [8] D. J. Sakrison, "On the role of the observer and a distortion measure in image transmission," *IEEE Trans. Commun.*, vol. COM-25, no. 11, pp. 1251–1267, Nov. 1977.
- [9] C. F. Hall, "Subjective evaluation of a perceptual quality metric," *Proc. SPIE*, vol. 310, pp. 200–204, 1981.
- [10] D. J. Granrath, "The role of human visual models in image processing," *Proc. IEEE*, vol. 69, no. 5, pp. 552–561, May 1981.
- [11] F. X. J. Lukas and Z. L. Budrikis, "Picture quality prediction based on a visual model," *IEEE Trans. Commun.*, vol. COM-30, no. 7, pp. 1679–1692, Jul. 1982.
- [12] N. B. Nill, "A visual model weighted cosine transform for image compression and quality assessment," *IEEE Trans. Commun.*, vol. COM-33, no. 6, pp. 551–557, Jun. 1985.
- [13] H. Marmolin, "Subjective MSE measures," *IEEE Trans. Syst., Man, Cybern.*, vol. SMC-16, no. 3, pp. 486–489, May/June 1986.
- [14] C. S. Stein, A. B. Watson, and L. E. Hitchner, "Psychophysical rating of image compression techniques," *Proc. SPIE*, vol. 1977, pp. 198–208, 1989.
- [15] J. A. Saghri, P. S. Cheatham, and A. Habibi, "Image quality measure based on a human visual system model," *Opt. Eng.*, vol. 28, no. 7, pp. 813–818, Jul. 1989.
- [16] G. G. Kuperman and B. L. Wilson, "Objective and subjective assessment of image compression algorithms," in *Proc. Soc. Information Display International Symp. Dig. Tech. Papers*, vol. 22, 1991, pp. 627–630.
- [17] J. Farrell, H. Trontelj, C. Rosenberg, and J. Wiseman, "Perceptual metrics for monochrome image compression," in *Proc. Soc. Information Display International Symp. Dig. Tech. Papers*, vol. 22, 1991, pp. 631–634.
- [18] N. B. Nill and B. H. Bouzas, "Objective image quality measures derived from digital image power spectra," *Opt. Eng.*, vol. 31, no. 4, pp. 813–825, Apr. 1992.
- [19] A. A. Webster, C. T. Jones, M. H. Pinson, S. D. Voran, and S. Wolf, "An objective video quality assessment system based on human perception," *Proc. SPIE*, vol. 1913, pp. 15–26, 1993.
- [20] S. Wolf, M. Pinson, C. Jones, and A. Webster, "A Summary of Methods of Measurement for Objective Video Quality Parameters Based on the Sobel Filtered Image and the Motion Difference Image," Inst. Telecomm. Sci., U.S. Dept. Commerce, Nat. Telecomm. Inf. Admin., Boulder, CO, Doc. T1A1.5/93–152, 1993.
- [21] H. Hamada and S. Namba, "A study on objective picture quality scales for pictures digitally encoded for broadcast," *IEICE Trans. Commun.*, vol. E77-B, no. 12, pp. 1480–1488, Dec. 1994.
- [22] W. Xu and G. Hauske, "Picture quality evaluation based on error segmentation," *Proc. SPIE*, vol. 2308, pp. 1454–1465, 1994.
- [23] A. M. Eskicioglu and P. S. Fisher, "The variance of the difference image: An alternative quality measure," in *Proc. Int. Picture Coding Symp.*, Sacramento, CA, Sep. 1994, pp. 88–91.
- [24] S. J. P. Westen, R. L. Lagendijk, and J. Biemond, "Perceptual image quality based on a multiple channel HVS model," in *Proc. Int. Conf. Acoustics, Speech, Signal Processing*, vol. 4, Detroit, MI, May 1995, pp. 2351–2354.
- [25] S. A. Karunasekera and N. G. Kingsbury, "A distortion measure for blocking artifacts in images based on human visual sensitivity," *IEEE Trans. Image Process.*, vol. 4, no. 6, pp. 713–724, Jun. 1995.
- [26] M. Kazubek, A. Przelaskowski, and T. Jamrógiewicz, "Quality measurement of compressed medical images: Block effect measures," in *Proc. 10th Nordic-Baltic Conf. Biomedical Engineering, Medical. Biological Engineering Computing*, 1996, pp. 235–236.
- [27] A. B. Watson, R. Borthwick, and M. Taylor, "Image quality and entropy masking," *Proc. SPIE*, vol. 3016, pp. 1–11, 1997.
- [28] M. P. Eckert and A. P. Bradley, "Perceptual quality metrics applied to still image compression," *Signal Process.*, vol. 70, pp. 177–200, 1998.
- [29] M. Miyahara, K. Kotani, and V. R. Algazi, "Compression of image coding techniques with a picture quality scale," *IEEE Trans. Commun.*, vol. COM-46, no. 9, pp. 1215–1226, Sep. 1998.
- [30] P. Franti, "Blockwise distortion measure for statistical and structural errors in digital images," *Signal Process.: Image Commun.*, vol. 13, pp. 89–98, 1998.
- [31] T. Eude and A. Mayache, "An evaluation of quality metrics for compressed images based on human visual sensitivity," in *Proc. 4th Int. Conf. Signal Processing*, vol. 1, Sep. 1998, pp. 779–782.
- [32] T. Eude, A. Mayache, and C. Milan, "A psychovisual quality metric based on multiscale texture analysis," *Proc. SPIE*, vol. 3644, pp. 235–244, 1999.
- [33] K. J. Hermiston and D. M. Booth, "Image quality measurement using integer wavelet transformations," in *Proc. Int. Conf. Image Processing*, Kobe, Japan, Oct. 1999, pp. 293–297.
- [34] Z. Wang and A. Bovik, "A universal image quality index," *IEEE Signal Process. Lett.*, vol. 9, no. 3, pp. 81–84, Mar. 2002.
- [35] T.-J. Chen, K.-S. CHuang, J. Wu, S. C. Chen, I.-M. Hwang, and M.-L. Jan, "A novel image quality index using moran I statistics," *Phys. Med. Biol.*, vol. 48, pp. N131–N137, 2003.
- [36] K. Hosaka, "A new picture quality evaluation method," in *Proc. Int. Picture Coding Symp.*, Tokyo, Japan, Apr. 1986, pp. 17–18.
- [37] P. M. Farrelle, *Recursive Block Coding for Image Data Compression*. New York: Springer-Verlag, 1990, pp. 104–154.
- [38] S. Daly, "The visible differences predictor: An algorithm for the assessment of image fidelity," *Proc. SPIE*, vol. 1616, pp. 2–15, 1992.
- [39] W. D. Abbott III, R. T. Kay, and R. J. Pieper, "Performance considerations for the application of the lossless browse and residual model," in *Proc. Space and Earth Science Data Compression Workshop*, Salt Lake City, UT, Apr. 1994, NASA Conf. Pub. 3258, pp. 43–54.
- [40] A. M. Eskicioglu and P. S. Fisher, "Image quality measures and their performance," *IEEE Trans. Commun.*, vol. 43, pp. 2959–2965, Dec. 1995.
- [41] A. M. Eskicioglu, "A multi-dimensional measure for image quality," presented at the Space and Earth Science Data Compression Workshop, Salt Lake City, UT, USA, Mar. 1995, JPL Pub. 95–8, pp. 83–92.
- [42] —, "An improved graphical quality measure for monochrome compressed images," in *Proc. Optical Engineering Midwest*, Chicago, IL, May 1995, pp. 692–701.

- [43] ———, “Application of multi-dimensional measures to reconstructed medical images,” *Opt. Eng.*, vol. 35, no. 3, pp. 778–785, Mar. 1996.
- [44] D. R. Fuhrmann, J. A. Baro, and J. R. Cox Jr., “Experimental evaluation of psychophysical distortion metrics for JPEG-encoded images,” *J. Electron. Imag.*, vol. 4, no. 4, pp. 397–406, Oct. 1996.
- [45] R. J. Beaton, “Quantitative models of image quality,” in *Proc. 27th Human Factors Soc. Annu. Meeting*, 1983, pp. 41–45.
- [46] Z. Wang, A. C. Bovik, H. R. Sheikh, and E. P. Simoncelli, “Image quality assessment: From error measurement to structural similarity,” *IEEE Trans. Image Process.*, vol. 13, no. 4, pp. 600–612, Apr. 2004.
- [47] A. Beghdadi and B. Pesquet-Popescu, “A new image distortion measure based on wavelet decomposition,” presented at the 7th ISSPA, Paris, France, Jul. 2003.
- [48] Z. Wang, A. C. Bovik, and B. L. Evans, “Blind measurement of blocking artifacts in images,” presented at the IEEE Inf. Conf. Image Processing, Vancouver, BC, Canada, Sep. 2000.
- [49] Z. Wang, H. R. Sheikh, and A. C. Bovik, “No-reference perceptual quality assessment of JPEG compressed images,” presented at the IEEE Inf. Conf. Image Processing, Rochester, NY, Sep. 2002.
- [50] A. C. Bovik and S. Liu, “DCT-domain blind measurement of blocking artifacts in DCT-coded images,” presented at the Inf. Conf. Acoustics, Speech, Signal Processing, Salt Lake City, UT, May 2001.
- [51] D. Kahaner, C. Moler, and S. Nash, *Numerical Methods and Software*. Englewood Cliffs, NJ: Prentice-Hall, 1989.
- [52] S. O. Aase, J. H. Husoy, and P. Waldemar, “A critique of SVD-based image coding systems,” in *Proc. IEEE Int. Symp. Circuits and Systems VLSI*, vol. 4, Orlando, FL, May 1999, pp. 13–16.
- [53] V. I. Gorodetski, L. J. Popyack, V. Samoilov, and V. A. Skormin, “SVD-based approach to transparent embedding data into digital images,” presented at the Int. Workshop Mathematical Methods, Models and Architectures for Computer Network Security, St. Petersburg, Russia, May 2001.
- [54] R. Liu and T. Tan, “A SVD-based watermarking scheme for protecting rightful ownership,” *IEEE Trans. Multimedia*, vol. 4, no. 1, pp. 121–128, Mar. 2002.
- [55] D. V. S. Chandra, “Digital image watermarking using singular value decomposition,” in *Proc. 45th IEEE Midwest Symp. Circuits and Systems*, Tulsa, OK, Aug. 2002, pp. 264–267.
- [56] *Final Report from the Video Quality Experts Group on the Validation of Objective Models of Video Quality Assessment*, A. M. Rohaly, J. Libert, P. Corriveau, and A. Webster, Eds., 2000.



Aleksandr Shnayderman received the B.S. degree from the Department of Computer and Information Science, Brooklyn College, The City University of New York, Brooklyn, in 2004.

Alexander Gusev received the B.S. degree from the Department of Computer and Information Science, Brooklyn College, The City University of New York, Brooklyn, in 2003.



Ahmet M. Eskicioglu received the B.S. degree from the Middle East Technical University, Ankara, Turkey, and the M.S. and Ph.D. degrees from the University of Manchester Institute of Science and Technology, Manchester, U.K.

He is with the Department of Computer and Information Science, Brooklyn College, The City University of New York, Brooklyn. He has actively participated in the development of several national and international standards for copy protection and conditional access in the U.S. and Europe, including the Content Scramble System (CSS) for DVD players, the Advanced Television Systems Committee (ATSC) conditional access system architecture, the Electronics Industries Alliance (EIA) National Renewable Security Standard (NRSS), and the European Union’s Digital Video Broadcasting (DVB) Content Protection and Copy Management (CPCM) System. He is the coauthor of two chapters in the *Multimedia Security Handbook* (CRC, 2004) and holds several patents on copy protection, conditional access, and digital interface protection. His teaching and research interests include data security, conditional access, digital rights management, copy protection, digital watermarking, and multimedia applications.